

Non-local topological electromagnetic phases of matter

Todd Van Mechelen and Zubin Jacob*

Birck Nanotechnology Center and Purdue Quantum Center,

Department of Electrical and Computer Engineering, Purdue University, West Lafayette, Indiana 47907, USA

In 2+1D, nonlocal topological electromagnetic phases are defined as atomic-scale media which host photonic monopoles in the bulk band structure and respect bosonic symmetries (e.g. time-reversal $\mathcal{T}^2 = +1$). Additionally, they support topologically protected spin-1 edge states, which are fundamentally different than spin- $\frac{1}{2}$ and pseudo-spin- $\frac{1}{2}$ edge states arising in fermionic and pseudo-fermionic systems. The striking feature of the edge state is that all electric and magnetic field components vanish at the boundary - in stark contrast to analogs of Jackiw-Rebbi domain wall states. This surprising open boundary solution of Maxwell's equations, dubbed the quantum gyroelectric effect [Phys. Rev. A **98**, 023842 (2018)], only occurs in the presence of temporal as well as spatial dispersion (nonlocality) and is the supersymmetric partner of the topological Dirac edge state where the spinor wave function completely vanishes at the boundary. In this paper, we generalize these topological electromagnetic phases beyond the continuum approximation to the exact lattice field theory of a periodic atomic crystal. To accomplish this, we put forth the concept of microscopic (nonlocal) photonic band structure of solids, analogous to the traditional theory of electronic band structure. Our definition of topological invariants and topological phases uses optical Bloch modes and can be applied to naturally occurring crystalline materials. For the photon propagating within a crystal, our theory shows that besides the Chern invariant $\mathfrak{C} \in \mathbb{Z}$, there are also symmetry-protected topological (SPT) invariants $\nu \in \mathbb{Z}_N$ which are related to the cyclic point group C_N of the crystal $\nu = \mathfrak{C} \bmod N$. Due to the rotational symmetries of light $\mathcal{R}(2\pi) = +1$, these SPT phases are manifestly bosonic and behave very differently from their fermionic counterparts $\mathcal{R}(2\pi) = -1$ encountered in conventional condensed matter systems. Remarkably, the nontrivial bosonic phases $\nu \neq 0$ are determined entirely from rotational (spin-1) eigenvalues of the photon at high-symmetry points in the Brillouin zone. Our work accelerates progress towards the discovery of bosonic phases of matter where the electromagnetic field within an atomic crystal exhibits topological properties.

I. INTRODUCTION

From a material science standpoint, all known topological phases of matter to date have been characterized by electronics [1]. This is true for both time-reversal broken phases - often called Chern insulators [2–5] and time-reversal unbroken phases - known as topological insulators [6, 7]. The signature of time-reversal broken phases is the quantum Hall conductivity $\sigma_{xy} = ne^2/h$, which is quantized in terms of the electronic Chern invariant $n \in \mathbb{Z}$ [8–10]. e being the elementary charge of the electron and h the Planck constant. Only recently has the idea of bosonic Hall conductivity and bosonic topological phases been put forth [11–19].

However, it should be emphasized that the traditional Hall conductivity [20, 21] only has topological significance, with respect to the electron, in the static $\omega = 0$ and local $k = 0$ limits of the electromagnetic field $\sigma_{xy}(0, 0) = ne^2/h$. At high frequency $\omega \neq 0$ and short wavelength $k \neq 0$, the Hall conductivity $\sigma_{xy}(\omega, \mathbf{k})$ acquires new physical meaning. We have shown that the electromagnetic field itself becomes topological [22, 23] and nonlocal Hall conductivity functions identically to a photonic mass [24–26] in the low-energy limit $\omega \approx 0$. These topological electromagnetic phases of matter depend on the *global* behavior of $\sigma_{xy}(\omega, \mathbf{k})$, over all frequencies and wave vectors.

As of yet, only the continuum topological theory of the quantum gyroelectric effect has been solved [22, 23]. Our goal is to extend this concept beyond the long wavelength ap-

proximation to the exact lattice field theory of optical Bloch waves. In this regime, we must consider not only the first spatial component $\sigma_{xy}(\omega, \mathbf{k}) = \sigma_{xy}(\omega, \mathbf{k}, 0)$ but all spatial harmonics of the crystal $\mathbf{g} \neq 0$, to infinite order,

$$J_x^{\text{Hall}}(\omega, \mathbf{k}) = \sum_{\mathbf{g}} \sigma_{xy}(\omega, \mathbf{k}, \mathbf{g}) E_y(\omega, \mathbf{k} + \mathbf{g}). \quad (1)$$

The electromagnetic field must be described to the same scale as the electronic wave functions, i.e. for photon momenta on the order of the lattice constant $ka = \pi$, with $a \approx 5 \text{ \AA}$. Since topological invariants are fundamentally global properties, these astronomically deep subwavelength fields actually play a role in the topological physics.

The idea of lattice topologies in electromagnetism was first proposed by Haldane [27, 28] in the context of photonic crystals [29–36]. These are artificial materials composed of two or more different constituents which form a macroscopic crystalline structure. A few notable examples are gyrotropic photonic crystals [29–31], Floquet topological insulators [37–39] and bianisotropic metamaterials [40–51]. Instead, we focus on the microscopic domain and utilize the periodicity of the atomic lattice itself. Thus, the photonic topological invariants in our theory are connected to the microscopic atomic lattice and not artificially engineered macroscopic structures. We stress that in the microscopic case, the electromagnetic theory is manifestly bosonic [52–54] (e.g. time-reversal $\mathcal{T}^2 = +1$) and characterizes topological phases of matter fundamentally distinct from known fermionic and pseudo-fermionic phases.

With that in mind, this paper is dedicated to solving two longstanding problems, which is of interest to both photonics and condensed matter physics. The first, is developing the rigorous theory of optical Bloch modes in natural crystal solids.

* zjacob@purdue.edu

This problem gained significant interest in the 60's and 70's in the context of spatial dispersion (nonlocality) as it lead to qualitatively new phenomena - such as natural optical activity (gyrotropy) [55–58]. The current paper builds on our recent discovery of the quantum gyroelectric effect [22, 23] where we have shown that nonlocality is also essential for topological phenomena and is a necessary ingredient in any long wavelength theory. However, since topological field theories are global constructs, a complete picture can only be achieved in the microscopic domain of Bloch waves. Most of the foundations have been summarized by Agronovich and Ginzburg in their seminal monograph on crystal optics [59]. Nevertheless, topological properties have never been tackled to date and a few fundamental quantities, such as the Bloch energy density, have not been defined.

This leads to the second problem - deriving the electromagnetic topological invariants of these systems given only the atomic lattice. We solve this problem and also provide a systematic bosonic classification of all 2+1D topological photonic matter. Utilizing the optical Bloch modes, we show that a Chern invariant $\mathfrak{C} \in \mathbb{Z}$ can be found for any two-dimensional crystal and characterizes distinct topological phases. We then go one step further and classify these topological phases with respect to the symmetry group of the crystal - the cyclic point groups C_N . These are known as symmetry-protected topological (SPT) phases [60–69] and the spin of the photon is critical to their definition. The rotational symmetries of light $\mathcal{R}(2\pi) = +1$ impart an intrinsically bosonic nature to these phases, which are fundamentally different than their fermionic counterparts $\mathcal{R}(2\pi) = -1$ encountered in conventional condensed matter systems. We illustrate this fact by directly comparing SPT bosonic and fermionic phases side-by-side. Our rigorous formalism of microscopic (nonlocal) photonic band structure provides an immediate parallel with the traditional theory of electronic band structure in crystal solids.

Remarkably, the SPT bosonic phases $\nu \in \mathbb{Z}_N$ of each point group C_N can be determined entirely from quantized spin-1 eigenvalues of the photon at high-symmetry points (HSPs) in the Brillouin zone. The SPT invariant $\nu = \mathfrak{C} \bmod N$ characterizes the electromagnetic Chern number up to a factor of N and is amenable to experiment as it is tied solely to the polarization state of the photon. The particular combination of quantized spin $m = \pm 1, 0$ and inversion $p = 1, 0$ eigenvalues at HSPs establishes all possible nontrivial phases $\nu \neq 0$. One strict constraint of this symmetry classification is that odd-valued Chern numbers $\mathfrak{C} \in 2\mathbb{Z} + 1$ are *forbidden* in nonmagnetic $C_{N=2,4,6}$ materials. The presence of inversion symmetry in these crystallographic point groups necessitates this condition.

This article is organized as follows. In Sec. II we develop the general formalism of 2+1D lattice electromagnetism. First we derive the generalized linear response function - accounting for spatiotemporal dispersion to infinite order in the crystal's spatial harmonics \mathbf{g} . Thereafter, we find the equivalent Hamiltonian that governs all light-matter Bloch excitations of the material. In Sec. III we study the discrete rotational symmetries (point groups) of the crystal and the implications on spin-1 quantization of the photon. The following Sec. IV

discusses the electromagnetic Chern number and its relationship to symmetry-protected topological (SPT) bosonic phases. The bosonic classification of each phase is related directly to integer quantization of the photon [Tab. I] and this is compared alongside their fermionic counterparts [Tab. II]. Sec. V presents our conclusions.

The focus of this paper is 2+1D topological electromagnetic (bosonic) phases of matter $\mathfrak{C} \neq 0$ which requires breaking time-reversal symmetry. These bosonic Chern insulators are ultimately related to nonlocal gyrotropic response (Hall conductivity) and show unidirectional, completely transverse electro-magnetic (TEM) edge states [22, 23]. However, time-reversal symmetric topological phenomena can arise in higher dimensional systems in the context of nonlocal magnetoelectricity [70]. These time-reversal symmetric phases possess counter-propagating TEM edge states and are interpreted as two copies of a bosonic Chern insulator. Features of topological phenomena, such as spin-momentum locking [71–75], have also been reported in conventional surface state problems - surface plasmon-polaritons (SPPs), Dyakonov waves, etc. However, these traditional surface properties are not connected to any topologically protected edge states or nontrivial phases.

Note: Due to the frequency of integral formulas, all differential elements are assumed to be correctly normalized, such as Fourier transforms $d\omega/\sqrt{2\pi} \rightarrow d\omega$ and Fourier series $e^{i\mathbf{g}\cdot\mathbf{r}}/\sqrt{V} \rightarrow e^{i\mathbf{g}\cdot\mathbf{r}}$, where V is the unit cell area of a crystal.

II. LATTICE ELECTROMAGNETISM

A. 2+1D electrodynamics

In this paper we focus on two-dimensional materials and the topological electromagnetic phases associated with them. The preliminaries for 2+1D electromagnetism can be found in Appendix A of Ref. [22]. Conveniently, the restriction to 2D limits the degrees of freedom of both the electromagnetic field and the induced response of the material, such that strictly transverse-magnetic (TM) waves propagate. The corresponding wave equation reads,

$$\mathcal{H}_0 f = i\partial_t g, \quad f = \begin{bmatrix} E_x \\ E_y \\ H_z \end{bmatrix}, \quad g = \begin{bmatrix} D_x \\ D_y \\ B_z \end{bmatrix}. \quad (2)$$

f is the TM polarization state of the electromagnetic field and the material response is captured by the displacement field g . $\mathcal{H}_0(\mathbf{p}) = \mathbf{p} \cdot \mathbf{S}$ are the vacuum Maxwell equations in real space and describe the dynamics of the free photon,

$$\mathcal{H}_0(\mathbf{p}) = p_x \hat{S}_x + p_y \hat{S}_y = \begin{bmatrix} 0 & 0 & -p_y \\ 0 & 0 & p_x \\ -p_y & p_x & 0 \end{bmatrix}. \quad (3)$$

$\mathbf{p} = -i\nabla$ is the two-dimensional momentum operator. \hat{S}_x and \hat{S}_y are spin-1 operators that satisfy the angular momentum

TABLE I. Summary of 2+1D topological electromagnetic (bosonic) phases. Symmetry-protected topological (SPT) bosonic phases exist in all cyclic point groups $C_{N=2,3,4,6}$. The continuous group C_∞ describes the long wavelength theory $k \approx 0$. The topological phases are characterized by their Chern invariant $\mathfrak{C} \in \mathbb{Z}$ and SPT invariant $\nu \in \mathbb{Z}_N$. These numbers are not independent - but intimately related by the symmetries of the crystal: $\nu = \mathfrak{C} \bmod N$. ν is protected by N -fold rotational symmetry and determines the Chern number up to a factor of N . The bosonic classification of ν represents the direct product of rotational eigenvalues $(z_N)^N = +1$ (roots of unity) of the electromagnetic field at high-symmetry points (HSPs) in the Brillouin zone. For the spin-1 photon, this classification is more intuitively understood in terms of quantized spin $m = \pm 1, 0$ and inversion $p = 1, 0$ eigenvalues at HSPs, which are related by $z_{N>2} = \exp(i2\pi m/N)$ and $z_2 = (-1)^p$.

Point group, C_N	Symmetry, \mathbb{Z}_N	Bosonic classification, $(z_N)^N = +1$	Boson SPT invariant, $\nu = \mathfrak{C} \bmod N$
C_1	-	-	-
C_2	\mathbb{Z}_2	$\exp(i2\pi\mathfrak{C}/2) = z_2(\Gamma)z_2(\mathbf{X})z_2(\mathbf{Y})z_2(\mathbf{M})$	$\nu = p(\Gamma) + p(\mathbf{X}) + p(\mathbf{Y}) + p(\mathbf{M}) \bmod 2$
C_3	\mathbb{Z}_3	$\exp(i2\pi\mathfrak{C}/3) = z_3(\Gamma)z_3(\mathbf{K})z_3(\mathbf{K}')$	$\nu = m(\Gamma) + m(\mathbf{K}) + m(\mathbf{K}') \bmod 3$
C_4	\mathbb{Z}_4	$\exp(i2\pi\mathfrak{C}/4) = z_4(\Gamma)z_4(\mathbf{M})z_2(\mathbf{Y})$	$\nu = m(\Gamma) + m(\mathbf{M}) + 2p(\mathbf{Y}) \bmod 4$
C_6	\mathbb{Z}_6	$\exp(i2\pi\mathfrak{C}/6) = z_6(\Gamma)z_3(\mathbf{K})z_2(\mathbf{M})$	$\nu = m(\Gamma) + 2m(\mathbf{K}) + 3p(\mathbf{M}) \bmod 6$
C_∞	\mathbb{Z}	$\exp(i\theta\mathfrak{C}) = z_\theta(0)z_\theta^*(\infty)$, $z_\theta = \exp(i\theta m)$	$\nu = \mathfrak{C} = m(0) - m(\infty)$

TABLE II. Summary of 2+1D SPT fermionic phases for comparison. The fermionic classification of ν represents the direct product of rotational eigenvalues $(w_N)^N = -1$ (roots of negative unity) of the spinor field at HSPs in the Brillouin zone. For the spin- $1/2$ electron, this classification is more intuitively understood in terms of quantized spin eigenvalues $m = \pm 1/2$ at HSPs, which are related by $w_N = \exp(i2\pi m/N)$.

Point group, C_N	Symmetry, \mathbb{Z}_N	Fermionic classification, $(w_N)^N = -1$	Fermion SPT invariant, $\nu = \mathfrak{C} \bmod N$
C_1	-	-	-
C_2	\mathbb{Z}_2	$\exp(i2\pi\mathfrak{C}/2) = w_2(\Gamma)w_2(\mathbf{X})w_2(\mathbf{Y})w_2(\mathbf{M})$	$\nu = m(\Gamma) + m(\mathbf{X}) + m(\mathbf{Y}) + m(\mathbf{M}) \bmod 2$
C_3	\mathbb{Z}_3	$\exp(i2\pi\mathfrak{C}/3) = -w_3(\Gamma)w_3(\mathbf{K})w_3(\mathbf{K}')$	$\nu = m(\Gamma) + m(\mathbf{K}) + m(\mathbf{K}') + 3/2 \bmod 3$
C_4	\mathbb{Z}_4	$\exp(i2\pi\mathfrak{C}/4) = -w_4(\Gamma)w_4(\mathbf{M})w_2(\mathbf{Y})$	$\nu = m(\Gamma) + m(\mathbf{M}) + 2m(\mathbf{Y}) + 2 \bmod 4$
C_6	\mathbb{Z}_6	$\exp(i2\pi\mathfrak{C}/6) = -w_6(\Gamma)w_3(\mathbf{K})w_2(\mathbf{M})$	$\nu = m(\Gamma) + 2m(\mathbf{K}) + 3m(\mathbf{M}) + 3 \bmod 6$
C_∞	\mathbb{Z}	$\exp(i\theta\mathfrak{C}) = w_\theta(0)w_\theta^*(\infty)$, $w_\theta = \exp(i\theta m)$	$\nu = \mathfrak{C} = m(0) - m(\infty)$

algebra $[\hat{S}_i, \hat{S}_j] = i\epsilon_{ijk}\hat{S}_k$,

$$\hat{S}_z = \begin{bmatrix} 0 & -i & 0 \\ i & 0 & 0 \\ 0 & 0 & 0 \end{bmatrix}. \quad (4)$$

Here, $(\hat{S}_z)_{ij} = -i\epsilon_{ijz}$ is the generator of rotations in the x - y plane and is represented by the antisymmetric matrix. In two dimensions, \hat{S}_z governs all rotational symmetries of the electromagnetic field [Fig. 1].

B. 2+1D linear response theory

The effective electromagnetic properties of a material are very accurately described by a linear response theory - assuming nonlinear interactions are negligible. This is true for low intensity light $|f| \lesssim 10^8$ V/m that is sufficiently weak compared to the atomic fields governing the binding of the crystal itself. Our goal is to characterize the entire topological field theory in this regime. With this in mind, the most general linear response of a 2D material is nonlocal in both space and time coordinates,

$$g(t, \mathbf{r}) = \int d^2\mathbf{r}' \int_{-\infty}^t dt' \mathcal{M}(t, t', \mathbf{r}, \mathbf{r}') f(t', \mathbf{r}'). \quad (5)$$

\mathcal{M} is the response function and compactly represents the constitutive relations in space-time,

$$\mathcal{M}(t, t', \mathbf{r}, \mathbf{r}') = \begin{bmatrix} \epsilon_{xx} & \epsilon_{xy} & \chi_x \\ \epsilon_{yx} & \epsilon_{yy} & \chi_y \\ \zeta_x & \zeta_y & \mu \end{bmatrix}. \quad (6)$$

Note that \mathcal{M} is a 3×3 dimensional matrix and we include all possible material responses as a generalization, for instance magnetism μ and magnetoelectricity χ_i, ζ_i .

If the properties of the crystal are not changing temporally (no external modulation), the response function is translationally invariant in time,

$$\begin{aligned} \mathcal{M}(t, t', \mathbf{r}, \mathbf{r}') &= \mathcal{M}(t - t', \mathbf{r}, \mathbf{r}') \\ &= \int d\omega \mathcal{M}(\omega, \mathbf{r}, \mathbf{r}') e^{-i\omega(t-t')}. \end{aligned} \quad (7)$$

Equation (7) implies energy conservation in Hermitian systems $\omega' = \omega$. However, a crystal is not translationally invariant in space - momentum is not conserved $\mathbf{k}' \neq \mathbf{k}$. Instead, the crystal is periodic and possesses *discrete* translational symmetry [59, 76],

$$\mathcal{M}(\omega, \mathbf{r}, \mathbf{r}') = \mathcal{M}(\omega, \mathbf{r} + \mathbf{R}, \mathbf{r}' + \mathbf{R}), \quad (8)$$

where \mathbf{R} is the primitive lattice vector of the crystal. This admits a Fourier decomposition in the spatial harmonics of the crystal \mathbf{g} ,

$$\mathcal{M}(\omega, \mathbf{r}, \mathbf{r}') = \sum_{\mathbf{g}} \mathcal{M}_{\mathbf{g}}(\omega, \mathbf{r} - \mathbf{r}') e^{-i\mathbf{r}' \cdot \mathbf{g}}, \quad (9)$$

with $\mathbf{g} \cdot \mathbf{R} \in 2\pi \mathbb{Z}$ arbitrary integer combinations of the reciprocal lattice vectors.

Due to nonlocality, it is necessary to convert to the reciprocal space,

$$\mathcal{M}(\omega, \mathbf{k}, \mathbf{k}') = \iint d^2\mathbf{r} d^2\mathbf{r}' \mathcal{M}(\omega, \mathbf{r}, \mathbf{r}') e^{-i\mathbf{k} \cdot \mathbf{r}} e^{i\mathbf{k}' \cdot \mathbf{r}'}. \quad (10)$$

$\mathcal{M}(\omega, \mathbf{k}, \mathbf{k}')$ determines the linear transformation properties of an input wave with momentum \mathbf{k}' to an output wave with momentum \mathbf{k} . In a periodic crystal, the momentum is conserved up to a reciprocal vector $\mathbf{k}' = \mathbf{k} + \mathbf{g}$ and represents a discrete spectrum,

$$\mathcal{M}(\omega, \mathbf{k}, \mathbf{k}') = \sum_{\mathbf{g}} \mathcal{M}_{\mathbf{g}}(\omega, \mathbf{k}) \delta^2(\mathbf{k} + \mathbf{g} - \mathbf{k}'). \quad (11)$$

$\delta^2(\mathbf{k} + \mathbf{g} - \mathbf{k}')$ is the momentum conserving delta function. Each Fourier element of the response function $\mathcal{M}_{\mathbf{g}}(\omega, \mathbf{k})$ determines the polarization dependent scattering amplitude from $\mathbf{k} \rightarrow \mathbf{k} + \mathbf{g}$. These are essentially the photonic structure factors of the two-dimensional crystal.

In this case, \mathbf{k} is the crystal momentum and is only uniquely defined within the Brillouin zone (BZ). Hence, the electromagnetic eigenstates of the medium are Bloch waves,

$$\begin{aligned} \mathcal{H}_0(\mathbf{k}) f_{\mathbf{k}} &= \omega \int d^2 \mathbf{k}' \mathcal{M}(\omega, \mathbf{k}, \mathbf{k}') f_{\mathbf{k}'} \\ &= \omega \sum_{\mathbf{g}} \mathcal{M}_{\mathbf{g}}(\omega, \mathbf{k}) f_{\mathbf{k}+\mathbf{g}}. \end{aligned} \quad (12)$$

$\mathcal{H}_0(\mathbf{k}) = \mathbf{k} \cdot \mathbf{S}$ are the vacuum Maxwell equations in momentum space. The Bloch photonic wave function $f(\mathbf{k}, \mathbf{r}) = \langle \mathbf{r} | f_{\mathbf{k}} \rangle$ corresponds to the net propagation of all $\mathbf{k} + \mathbf{g}$ scattered waves in the medium,

$$f(\mathbf{k}, \mathbf{r}) = \sum_{\mathbf{g}} f_{\mathbf{k}+\mathbf{g}} e^{i\mathbf{g} \cdot \mathbf{r}}, \quad (13)$$

where $f(\mathbf{k}, \mathbf{r} + \mathbf{R}) = f(\mathbf{k}, \mathbf{r})$ is periodic in the crystal lattice. Note that Eq. (12) and (13) reduce to the continuum theory [22] when considering only the 0th order harmonic $\mathbf{g} = 0$.

C. Generalized response function

Nevertheless, Eq. (12) poses a few serious problems; it does not represent a proper first-order in time Hamiltonian since all harmonics of the response function $\mathcal{M}_{\mathbf{g}}(\omega, \mathbf{k})$ depend on the eigenvalue ω . Moreover, it is not evident that the Bloch waves in Eq. (13) are normalizable, as the system contains complex spatial and temporal dispersion. Due to these issues, it is advantageous to return to the more general form of $\mathcal{M}(\omega, \mathbf{k}, \mathbf{k}')$ without assuming discrete translational symmetry. This will allow us to derive very robust properties of the response function that can also be applied to amorphous materials or quasicrystals.

First, we demand Hermiticity,

$$\mathcal{M}(\omega, \mathbf{k}, \mathbf{k}') = \mathcal{M}^\dagger(\omega, \mathbf{k}', \mathbf{k}), \quad (14)$$

such that the response is lossless. To account for normalizable electromagnetic waves, the energy density must be positive definite for all ω ,

$$U(\omega) = \iint d^2 \mathbf{k} d^2 \mathbf{k}' f_{\mathbf{k}}^\dagger \bar{\mathcal{M}}(\omega, \mathbf{k}, \mathbf{k}') f_{\mathbf{k}'} > 0, \quad (15)$$

where $\bar{\mathcal{M}}$ describes the inner product space in a dispersive medium,

$$\bar{\mathcal{M}}(\omega, \mathbf{k}, \mathbf{k}') = \frac{\partial}{\partial \omega} [\omega \mathcal{M}(\omega, \mathbf{k}, \mathbf{k}')]. \quad (16)$$

Notice that $U(\omega) = U^*(\omega)$ is only real-valued when \mathcal{M} is Hermitian. For realistic materials, the energy density is also stable at static equilibrium $\omega = 0$,

$$U(0) = \iint d^2 \mathbf{k} d^2 \mathbf{k}' f_{\mathbf{k}}^\dagger \mathcal{M}(0, \mathbf{k}, \mathbf{k}') f_{\mathbf{k}'} > 0, \quad (17)$$

with $\mathcal{M}(0, \mathbf{k}, \mathbf{k}') = \bar{\mathcal{M}}(0, \mathbf{k}, \mathbf{k}')$ at zero frequency. To ensure the electromagnetic field is real-valued, i.e. represents a neutral particle, we always require the reality condition,

$$\mathcal{M}(\omega, \mathbf{k}, \mathbf{k}') = \mathcal{M}^*(-\omega, -\mathbf{k}, -\mathbf{k}'). \quad (18)$$

Furthermore, the response is transparent at high frequency $\omega \rightarrow \infty$, as the material cannot respond to sufficiently fast temporal oscillations,

$$\lim_{\omega \rightarrow \infty} \mathcal{M}(\omega, \mathbf{k}, \mathbf{k}') = \mathbb{1}_3 \delta_{\mathbf{k}-\mathbf{k}'}. \quad (19)$$

$\mathbb{1}_3$ is the 3×3 identity matrix and $\delta_{\mathbf{k}-\mathbf{k}'}^2 = \delta^2(\mathbf{k} - \mathbf{k}')$ is the momentum conserving delta function. Lastly, the response must be causal and satisfy the Kramers-Kronig relations.

Combining all the above criteria, we find that \mathcal{M} can always be decomposed as a discrete summation of oscillators [27, 47, 77],

$$\mathcal{M}(\omega, \mathbf{k}, \mathbf{k}') = \mathbb{1}_3 \delta_{\mathbf{k}-\mathbf{k}'}^2 - \sum_{\alpha} \int d^2 \mathbf{k}'' \frac{\mathcal{C}_{\alpha \mathbf{k}'' \mathbf{k}}^\dagger \mathcal{C}_{\alpha \mathbf{k}'' \mathbf{k}'}}{\omega_{\alpha \mathbf{k}''} (\omega - \omega_{\alpha \mathbf{k}''})}. \quad (20)$$

Any Hermitian (lossless) response function can be expressed in this form. Equation (20) is easily extended to 3D materials but our focus is on 2D topological field theories. In this case, α labels an arbitrary bosonic excitation in the material, such as an exciton or phonon, which couples linearly to the electromagnetic fields via the 3×3 tensor,

$$\mathcal{C}_{\alpha}(\mathbf{k}, \mathbf{k}') = \iint d^2 \mathbf{r} d^2 \mathbf{r}' \mathcal{C}_{\alpha}(\mathbf{r}, \mathbf{r}') e^{-i\mathbf{k} \cdot \mathbf{r}} e^{i\mathbf{k}' \cdot \mathbf{r}'}. \quad (21)$$

$\omega_{\alpha \mathbf{k}}$ is the resonant energy of the oscillator and corresponds to a first-order pole of the response function. Notice that \mathcal{M} itself contains an integral over \mathbf{k}'' . Microscopically, this constitutes the overlap with the electronic momentum to infinitesimally small scale $k \rightarrow \infty$.

Substituting Eq. (20) into Eq. (15), we can exchange the order of integration $U(\omega) = \int d^2 \mathbf{k} U(\omega, \mathbf{k})$ and define,

$$U(\omega, \mathbf{k}) = |f_{\mathbf{k}}|^2 + \sum_{\alpha} \left| \int d^2 \mathbf{k}' \frac{\mathcal{C}_{\alpha \mathbf{k} \mathbf{k}'} f_{\mathbf{k}'}}{\omega - \omega_{\alpha \mathbf{k}}} \right|^2 > 0, \quad (22)$$

which is positive definite for all ω and \mathbf{k} . Equation (22) is the generalized inner product for the electromagnetic field and represents the energy density at an arbitrary frequency and wave vector. We will now show that Eq. (20) is derived from a first-order Hamiltonian.

D. Generalized Hamiltonian

To find the corresponding Hamiltonian, we expand the response function \mathcal{M} in terms of three-component matter oscillators ψ_α . These represent internal polarization and magnetization modes of the material,

$$\omega\psi_{\alpha\mathbf{k}} = \omega_{\alpha\mathbf{k}}\psi_{\alpha\mathbf{k}} + \int d^2\mathbf{k}' C_{\alpha\mathbf{k}\mathbf{k}'} f_{\mathbf{k}'}. \quad (23)$$

$$H(\mathbf{k}, \mathbf{k}') = \begin{bmatrix} \mathcal{H}_0(\mathbf{k})\delta_{\mathbf{k}-\mathbf{k}'}^2 + \sum_\alpha \int \frac{d^2\mathbf{k}''}{\omega_{\alpha\mathbf{k}''}} C_{\alpha\mathbf{k}''\mathbf{k}}^\dagger C_{\alpha\mathbf{k}''\mathbf{k}'} & C_{1\mathbf{k}'\mathbf{k}}^\dagger & C_{2\mathbf{k}'\mathbf{k}}^\dagger & \cdots \\ C_{1\mathbf{k}\mathbf{k}'} & \omega_{1\mathbf{k}}\delta_{\mathbf{k}-\mathbf{k}'}^2 & 0 & \cdots \\ C_{2\mathbf{k}\mathbf{k}'} & 0 & \omega_{2\mathbf{k}}\delta_{\mathbf{k}-\mathbf{k}'}^2 & \cdots \\ \vdots & \vdots & \vdots & \ddots \end{bmatrix}, \quad (25)$$

which is manifestly Hermitian $H(\mathbf{k}, \mathbf{k}') = H^\dagger(\mathbf{k}', \mathbf{k})$.

We now define $u_{\mathbf{k}}$ as the generalized state vector of the electromagnetic problem; accounting for the photon $f_{\mathbf{k}}$ and all possible internal excitations $\psi_{\alpha\mathbf{k}}$,

$$\int d^2\mathbf{k}' H_{\mathbf{k}\mathbf{k}'} u_{\mathbf{k}'} = \omega u_{\mathbf{k}}, \quad u_{\mathbf{k}} = \begin{bmatrix} f_{\mathbf{k}} \\ \psi_{1\mathbf{k}} \\ \psi_{2\mathbf{k}} \\ \vdots \end{bmatrix}, \quad (26)$$

which is a first-order wave equation. Notice that contraction of $u_{\mathbf{k}}$ naturally reproduces the energy density [Eq. (22)] upon summation over all degrees of freedom,

$$\begin{aligned} u_{\mathbf{k}}^\dagger u_{\mathbf{k}} &= |f_{\mathbf{k}}|^2 + \sum_\alpha |\psi_{\alpha\mathbf{k}}|^2 = U(\omega, \mathbf{k}) \\ &= |f_{\mathbf{k}}|^2 + \sum_\alpha \left| \int d^2\mathbf{k}' \frac{C_{\alpha\mathbf{k}\mathbf{k}'} f_{\mathbf{k}'}}{(\omega - \omega_{\alpha\mathbf{k}})} \right|^2. \end{aligned} \quad (27)$$

The complete set of eigenvectors and eigenvalues is represented by $u_{\mathbf{k}}$. We must define all relevant electromagnetic quantities in terms of this generalized state vector.

E. Crystal Hamiltonian

We are now ready to enforce crystal periodicity. Instead of expanding \mathcal{M} directly, we utilize the periodicity of the coupling tensors $\mathcal{C}_\alpha(\mathbf{r}, \mathbf{r}') = \mathcal{C}_\alpha(\mathbf{r} + \mathbf{R}, \mathbf{r}' + \mathbf{R})$, which is a discrete spectrum in \mathbf{g} ,

$$C_\alpha(\mathbf{k}, \mathbf{k}') = \sum_{\mathbf{g}} C_{\alpha\mathbf{g}}(\mathbf{k}) \delta^2(\mathbf{k} + \mathbf{g} - \mathbf{k}'). \quad (28)$$

$C_{\alpha\mathbf{g}}(\mathbf{k})$ tells us the scattering amplitude of a photon $f_{\mathbf{k}}$ with momentum \mathbf{k} into an internal mode of the material $\psi_{\alpha\mathbf{k}+\mathbf{g}}$ at

Substituting Eq. (23) and (20) into Eq. (12) we obtain,

$$\begin{aligned} \omega f_{\mathbf{k}} &= \mathcal{H}_0(\mathbf{k}) f_{\mathbf{k}} + \sum_\alpha \iint \frac{d^2\mathbf{k}'' d^2\mathbf{k}'}{\omega_{\alpha\mathbf{k}''}} C_{\alpha\mathbf{k}''\mathbf{k}}^\dagger C_{\alpha\mathbf{k}''\mathbf{k}'} f_{\mathbf{k}'} \\ &+ \sum_\alpha \int d^2\mathbf{k}' C_{\alpha\mathbf{k}'\mathbf{k}}^\dagger \psi_{\alpha\mathbf{k}'}. \end{aligned} \quad (24)$$

The first two terms of Eq. (24) represent the vacuum equations and self-energy of the electromagnetic field. The third term is the linear coupling to the oscillators. Combining Eq. (23) and (24) into a single algebraic matrix, we write the generalized Hamiltonian $H(\mathbf{k}, \mathbf{k}')$ as,

momentum $\mathbf{k} + \mathbf{g}$, and vice versa. The crystal Hamiltonian accounts for all such scattering events,

$$H(\mathbf{k}, \mathbf{k}') = \sum_{\mathbf{g}} H_{\mathbf{g}}(\mathbf{k}) \delta^2(\mathbf{k} + \mathbf{g} - \mathbf{k}'), \quad (29)$$

with Hermiticity $H_{\mathbf{g}}(\mathbf{k}) = H_{-\mathbf{g}}^\dagger(\mathbf{k} + \mathbf{g})$ satisfied by definition. Note, the resonant energies $\omega_\alpha(\mathbf{k} + \mathbf{g}) = \omega_\alpha(\mathbf{k})$ are generally periodic in \mathbf{k} , since they correspond to energy gaps in the electronic band structure. However, we do not need to assume this to define the optical Bloch excitations. A periodic coupling is sufficient.

The quasiparticle eigenstates of this Hamiltonian describe the complete spectrum of Bloch waves,

$$\sum_{\mathbf{g}} H_{\mathbf{g}}(\mathbf{k}) u_{n\mathbf{k}+\mathbf{g}} = \omega_{n\mathbf{k}} u_{n\mathbf{k}}, \quad \omega_n(\mathbf{k} + \mathbf{g}) = \omega_n(\mathbf{k}), \quad (30)$$

and the eigenenergies $\omega_{n\mathbf{k}}$ are periodic Bloch bands. n labels a particular energy band of the material with its associated Bloch eigenstate $|u_{n\mathbf{k}}\rangle$. The total wave function $|u_{n\mathbf{k}}\rangle$ contains the photon $|f_{n\mathbf{k}}\rangle$ and all internal degrees of freedom describing the linear response $|\psi_{n\alpha\mathbf{k}}\rangle$. This is expressed compactly in the Fourier basis $u_n(\mathbf{k}, \mathbf{r}) = \langle \mathbf{r} | u_{n\mathbf{k}} \rangle$,

$$u_n(\mathbf{k}, \mathbf{r}) = \sum_{\mathbf{g}} u_{n\mathbf{k}+\mathbf{g}} e^{i\mathbf{g}\cdot\mathbf{r}}, \quad u_{n\mathbf{k}+\mathbf{g}} = \begin{bmatrix} f_{n\mathbf{k}+\mathbf{g}} \\ \psi_{n1\mathbf{k}+\mathbf{g}} \\ \psi_{n2\mathbf{k}+\mathbf{g}} \\ \vdots \end{bmatrix}, \quad (31)$$

where $u_n(\mathbf{k}, \mathbf{r} + \mathbf{R}) = u_n(\mathbf{k}, \mathbf{r})$ is periodic in the crystal lattice. In this basis, $|u_{n\mathbf{k}}\rangle$ is normalized to the energy density

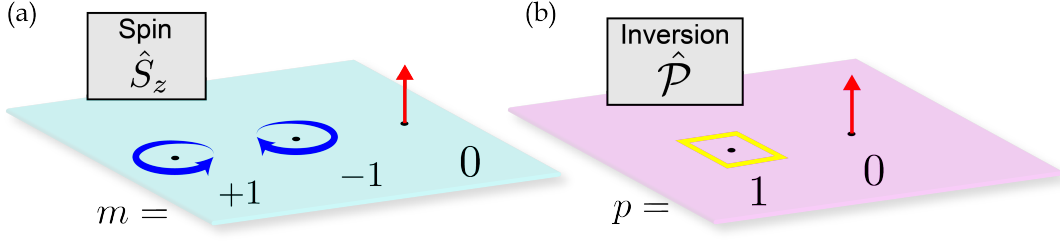


FIG. 1. (a) Quantized spin-1 eigenstates $\hat{S}_z \mathbf{e} = m\mathbf{e}$, with $m = \pm 1, 0$ integer quantum numbers. $m = \pm 1$ labels eigenstates of right- and left-handed rotations $\mathbf{e}_{\pm} = \frac{1}{\sqrt{2}}(1, \pm i, 0)$, which correspond to electric resonances. $m = 0$ is a magnetic resonance and represents the irrotational spin-0 state $\mathbf{e}_0 = (0, 0, 1)$. (b) Quantized inversion eigenstates $\hat{P} \mathbf{e} = (-1)^p \mathbf{e}$, with $p = 1, 0$ integer quantum numbers. $p = 1$ labels the odd inversion state $\mathbf{e}_1 = a\mathbf{e}_+ + b\mathbf{e}_-$, which can be any linear superposition of electric resonances. The even inversion state $p = m = 0$ is simply the magnetic resonance \mathbf{e}_0 .

as,

$$\begin{aligned} 1 &= \langle u_{n\mathbf{k}} | u_{n\mathbf{k}} \rangle = \sum_{\mathbf{g}} u_{n\mathbf{k}+\mathbf{g}}^\dagger u_{n\mathbf{k}+\mathbf{g}} \\ &= \sum_{\mathbf{g}\mathbf{g}'} f_{n\mathbf{k}+\mathbf{g}}^\dagger \bar{\mathcal{M}}_{\mathbf{g}'-\mathbf{g}}(\omega_{n\mathbf{k}}, \mathbf{k} + \mathbf{g}) f_{n\mathbf{k}+\mathbf{g}'}. \end{aligned} \quad (32)$$

The bra-ket notation $\langle | \rangle$ implies spatial integration over the 2D unit cell, which is orthogonal to the Kronecker delta in the Fourier basis $\langle \mathbf{g} | \mathbf{g}' \rangle = \delta_{\mathbf{g}\mathbf{g}'}$. $\bar{\mathcal{M}}_{\mathbf{g}}(\omega, \mathbf{k}) = \partial_\omega [\omega \mathcal{M}_{\mathbf{g}}(\omega, \mathbf{k})]$ is the contribution to the energy density arising from each spatial harmonic of the crystal.

Finally, the eigenenergies $\omega_{n\mathbf{k}}$ are the n nontrivial roots of the characteristic wave equation,

$$\mathcal{H}_0(\mathbf{k}) f_{n\mathbf{k}} = \omega_{n\mathbf{k}} \sum_{\mathbf{g}} \mathcal{M}_{\mathbf{g}}(\omega_{n\mathbf{k}}, \mathbf{k}) f_{n\mathbf{k}+\mathbf{g}}, \quad (33)$$

which generates all possible photonic bands of the crystal. Note, the response function $\mathcal{M}_{\mathbf{g}}(\omega, \mathbf{k})$ is now expressed in terms of $\mathcal{C}_{\alpha\mathbf{g}}(\mathbf{k})$ and describes the net summation of all scattering and back-scattering events in the material,

$$\mathcal{M}_{\mathbf{g}}(\omega, \mathbf{k}) = \mathbb{1}_3 \delta_{\mathbf{g}} - \sum_{\alpha\mathbf{g}'} \frac{C_{\alpha-\mathbf{g}'}^\dagger(\mathbf{k} + \mathbf{g}') C_{\alpha\mathbf{g}-\mathbf{g}'}(\mathbf{k} + \mathbf{g}')}{\omega_{\alpha\mathbf{k}+\mathbf{g}'}(\omega - \omega_{\alpha\mathbf{k}+\mathbf{g}'})}. \quad (34)$$

This proves that the wave equation is derived from a first-order Hamiltonian, has real eigenvalues $\omega = \omega_{n\mathbf{k}}$ for all momenta, and is normalizable in terms of $|u_{n\mathbf{k}}\rangle$.

III. DISCRETE ROTATIONAL SYMMETRY

A. Point groups in 2D

Point groups are the discrete analogs of continuous rotations and reflections. They represent the number of ways the atomic lattice can be transformed into itself [78, 79]. Due to the crystallographic restriction theorem (CRT), there are ten such point groups in 2D. The first five are the cyclic groups

C_N ,

$$C_1, C_2, C_3, C_4, C_6. \quad (35)$$

For instance, C_3 implies threefold cyclic symmetry while C_1 is no symmetry. The last five are the dihedral groups D_N ,

$$D_1, D_2, D_3, D_4, D_6. \quad (36)$$

The dihedral group D_N contains C_N plus reflections. However, it can be proven that the Chern number for all D_N point groups vanish [63]. Therefore, we concern ourselves with only the cyclic groups C_N . The Brillouin zone of each point group is displayed in Fig. 2.

The defining characteristic of each cyclic group is the fermionic or bosonic representation. When we rotate the fields by 2π , we take the particle into itself and acquire a phase,

$$\mathcal{R}(2\pi) = (-1)^F. \quad (37)$$

F is twice the total spin of particle, or equivalently, the fermion number. Fermions with half-integer spin are anti-symmetric under rotations $\mathcal{R}(2\pi) = -1$, while bosons with integer spin are symmetric $\mathcal{R}(2\pi) = +1$. Depending on the symmetries of the lattice, the topology fundamentally changes for fermions and bosons. We will understand the implications this has for spin-1 photons.

B. Spin-1 discrete symmetries

If the two-dimensional crystal belongs to a cyclic point group C_N , the Hamiltonian possesses discrete rotational symmetry about z ,

$$\mathcal{R}^{-1} H_{\mathcal{R}\mathbf{g}}(\mathcal{R}\mathbf{k}) \mathcal{R} = H_{\mathbf{g}}(\mathbf{k}), \quad \omega_n(\mathcal{R}\mathbf{k}) = \omega_n(\mathbf{k}), \quad (38)$$

where \mathcal{R} is a rotation in C_N . Note that \mathcal{R} is diagonal in u , meaning the photon and each oscillator is rotated individually, $f \rightarrow \mathcal{R}f$ and $\psi_\alpha \rightarrow \mathcal{R}\psi_\alpha$. This symmetry is endowed by the coupling tensors, which dictates the degrees of freedom of the material response,

$$\mathcal{R}^{-1} C_{\alpha\mathcal{R}\mathbf{g}}(\mathcal{R}\mathbf{k}) \mathcal{R} = C_{\alpha\mathbf{g}}(\mathbf{k}), \quad \omega_\alpha(\mathcal{R}\mathbf{k}) = \omega_\alpha(\mathbf{k}). \quad (39)$$

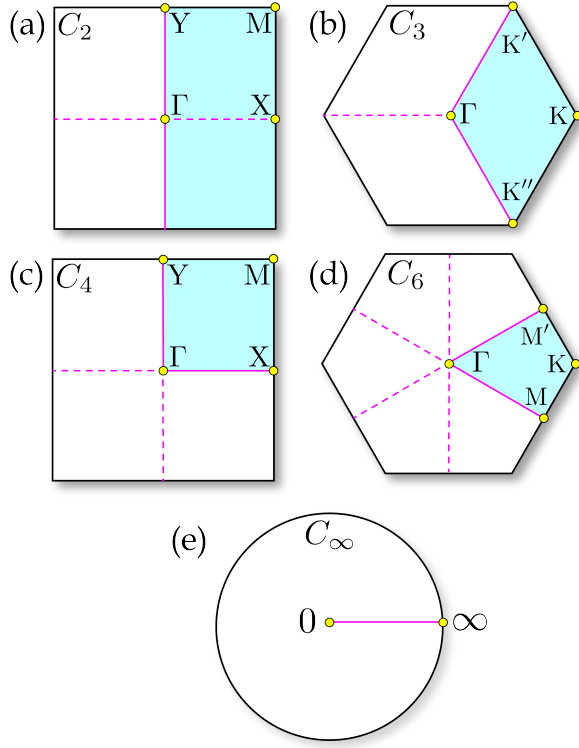


FIG. 2. Brillouin zone of each cyclic point group C_N . (a), (b), (c), (d), and (e) correspond to $N = 2, 3, 4, 6$, and ∞ respectively. Due to rotational symmetry, the total Brillouin zone is equivalent to N copies of the irreducible Brillouin zone (IBZ), which is represented by the blue quadrant. For continuous symmetry $N = \infty$, this is simply a line. The yellow circles label high-symmetry points $\mathcal{R}\mathbf{k}_p = \mathbf{k}_p$ where the Hamiltonian is invariant under a discrete rotation \mathcal{R} . At these specific momenta, a Bloch photonic wave function $|f_n(\mathbf{k}_p)\rangle$ possesses quantized spin $m_n(\mathbf{k}_p) = \pm 1, 0$ or inversion $p_n(\mathbf{k}_p) = 1, 0$ eigenvalues. Since m and p are discrete quantum numbers, their values cannot vary continuously if the crystal symmetry is preserved - they can only be changed at a topological phase transition.

After summation over all $C_{\text{og}}(\mathbf{k})$, we can prove that the response function transforms identically under such a rotation,

$$\mathcal{R}^{-1} \mathcal{M}_{\mathcal{R}\mathbf{g}}(\omega, \mathcal{R}\mathbf{k}) \mathcal{R} = \mathcal{M}_{\mathbf{g}}(\omega, \mathbf{k}). \quad (40)$$

Therefore, the photon inherits all symmetries of the crystal.

Any rotation, continuous or discrete, can be expressed as the exponential of the spin-1 generator (\hat{S}_z) $_{ij} = -i\epsilon_{ijz}$,

$$\mathcal{R}_N = \exp(i\theta_N \hat{S}_z) = \begin{bmatrix} \cos \theta_N & \sin \theta_N & 0 \\ -\sin \theta_N & \cos \theta_N & 0 \\ 0 & 0 & 1 \end{bmatrix}. \quad (41)$$

In this case, $\theta_N = 2\pi/N$ is an N -fold rotation with the same order as the point group C_N . Since the cyclic groups are Abelian, all elements in the group can be found from repeated applications $\mathcal{R}(M\theta_N) = \mathcal{R}_N^M$, where $M = 1, 2, \dots, N-1$ is an integer. We stress that every cyclic group for the photon is a vector representation, which is *bosonic*,

$$\mathcal{R}(2\pi) = \mathcal{R}(N\theta_N) = \mathcal{R}_N^N = +\mathbb{1}_3. \quad (42)$$

The electromagnetic field returns in phase under cyclic revolution.

1. Spin-1 eigenstates

Eigenstates of a rotation \mathcal{R}_N are simultaneous eigenstates of the spin \hat{S}_z . These constitute electromagnetic waves with quantized polarization, transverse to the x - y plane,

$$\mathcal{R}_N \mathbf{e} = z_N \mathbf{e}, \quad \hat{S}_z \mathbf{e} = m \mathbf{e}, \quad (43a)$$

where the eigenvalues are related by,

$$z_N = \exp(i\theta_N m), \quad (z_N)^N = +1. \quad (43b)$$

z_N are the eigenvalues of \mathcal{R}_N and represent the N th roots of unity. m are the corresponding spin eigenvalues of \hat{S}_z . For photons, the spin is an integer $m = \pm 1, 0$ and takes one of three discrete values. First, we have the $m = \pm 1$ spin states,

$$\mathbf{e}_{\pm} = \frac{1}{\sqrt{2}} \begin{bmatrix} 1 \\ \pm i \\ 0 \end{bmatrix}, \quad \hat{S}_z \mathbf{e}_{\pm} = \pm \mathbf{e}_{\pm}. \quad (44)$$

\mathbf{e}_{\pm} are electric resonances ($H_z = 0$) and denote eigenstates of right- or left-handed rotations. Second, we have the $m = 0$ spin state, which is a magnetic resonance ($E_i = 0$) and designates the irrotational eigenstate,

$$\mathbf{e}_0 = \begin{bmatrix} 0 \\ 0 \\ 1 \end{bmatrix}, \quad \hat{S}_z \mathbf{e}_0 = 0. \quad (45)$$

Notice the $m = 0$ state generates the same eigenvalue $z_N = +1$ regardless of the rotation. A visualization of the spin-1 eigenstates is presented in Fig. 1(a).

2. Spin-1 inversion eigenstates

For $N = 2$, a rotation is equivalent to inversion $\mathcal{R}_2 = \hat{\mathcal{P}} = \text{dgl}[-1, -1, 1]$. Note though, since a rotation by π or $-\pi$ is identical for bosons, \mathbf{e}_+ and \mathbf{e}_- possess the same inversion eigenvalues. This means we can only define two unique inversion states $p = 1, 0$ with two discrete values,

$$\hat{\mathcal{P}} \mathbf{e} = z_2 \mathbf{e} = (-1)^p \mathbf{e}, \quad (46)$$

which act on the spin states as,

$$\hat{\mathcal{P}} \mathbf{e}_{\pm} = (-1)^1 \mathbf{e}_{\pm}, \quad \hat{\mathcal{P}} \mathbf{e}_0 = (-1)^0 \mathbf{e}_0. \quad (47)$$

Both \mathbf{e}_{\pm} spin eigenstates are odd under inversion. Therefore, any linear superposition $\mathbf{e}_1 = a\mathbf{e}_+ + b\mathbf{e}_-$ is also a valid eigenstate, with eigenvalue $p = 1$. On the other hand, the magnetic \mathbf{e}_0 eigenstate is even under inversion, with eigenvalue $p = m = 0$. A depiction of the inversion eigenstates is presented in Fig. 1(b).

C. High-symmetry points

At an arbitrary crystal momentum \mathbf{k} , the Bloch wave functions $|u_{n\mathbf{k}}\rangle$ are not eigenstates of any particular rotation \mathcal{R} . However, there are specific points in the Brillouin zone where \mathbf{k} is invariant under,

$$\mathcal{R}\mathbf{k}_p = \mathbf{k}_p. \quad (48)$$

This is because the crystal momentum only differs by a lattice translation at these points $\mathcal{R}\mathbf{k}_p = \mathbf{k}_p + \mathbf{g}$, which leaves a periodic wave function unchanged (up to a phase),

$$|u_n(\mathcal{R}\mathbf{k}_p)\rangle = |u_n(\mathbf{k}_p + \mathbf{g})\rangle = |u_n(\mathbf{k}_p)\rangle. \quad (49)$$

These are called *high-symmetry points* (HSPs); they occur at the center and certain vertices of the Brillouin zone. The crystal Hamiltonian is *rotationally invariant* at these momenta. Therefore, the wave functions are simultaneous eigenstates of \mathcal{R} at HSPs,

$$\mathcal{R}|u_n(\mathbf{k}_p)\rangle = z_n(\mathbf{k}_p)|u_n(\mathbf{k}_p)\rangle. \quad (50)$$

Here, $z_n(\mathbf{k}_p)$ is the eigenvalue of \mathcal{R} at \mathbf{k}_p for the n th band. Depending on the point group and the precise HSP, $z_n(\mathbf{k}_p) = z_{N,n}(\mathbf{k}_p)$ can represent any N th root of unity. We will now prove unequivocally that knowing the eigenstate of the photon at HSPs $|f_n(\mathbf{k}_p)\rangle$ is sufficient to determine $z_n(\mathbf{k}_p)$.

D. Quantization of the photon

Since \mathcal{R} is *diagonal* in the total Bloch function $|u_{n\mathbf{k}}\rangle$, it follows immediately that the rotational eigenvalue $z_n(\mathbf{k}_p)$ is identical for the photon $|f_n(\mathbf{k}_p)\rangle$ and all internal polarization modes $|\psi_{n\alpha}(\mathbf{k}_p)\rangle$. We can prove this another way by evaluating the expectation value, which contracts over all degrees of freedom,

$$z_n(\mathbf{k}_p) = \langle u_n(\mathbf{k}_p) | \mathcal{R} | u_n(\mathbf{k}_p) \rangle. \quad (51)$$

Utilizing the linear response theory [Eq. (23)] and the commutation properties of $\mathcal{C}_{\alpha\mathbf{g}}(\mathbf{k}_p)$ at HSPs, this can be simplified to yield,

$$z_n(\mathbf{k}_p) = \sum_{\mathbf{g}\mathbf{g}'} f_{n\mathbf{k}_p+\mathbf{g}}^\dagger \bar{\mathcal{M}}_{\mathbf{g}'-\mathbf{g}}(\omega_{n\mathbf{k}_p}, \mathbf{k}_p + \mathbf{g}) \mathcal{R} f_{n\mathbf{k}_p+\mathbf{g}'}. \quad (52)$$

The normalization condition [Eq. (32)] is satisfied by definition at \mathbf{k}_p . For Eq. (52) to hold simultaneously, each spatial harmonic $\mathcal{R}f_{n\mathbf{k}_p+\mathbf{g}} = z_n(\mathbf{k}_p)f_{n\mathbf{k}_p+\mathbf{g}}$ must correspond to the same polarization state - they only differ in relative magnitude. Hence, $z_n(\mathbf{k}_p)$ is clearly the eigenvalue of the Bloch photonic wave function,

$$\mathcal{R}|f_n(\mathbf{k}_p)\rangle = z_n(\mathbf{k}_p)|f_n(\mathbf{k}_p)\rangle. \quad (53)$$

Consequently, the electromagnetic field $|f_n(\mathbf{k}_p)\rangle$ is a quantized spin $m_n(\mathbf{k}_p) = \pm 1, 0$ or inversion $p_n(\mathbf{k}_p) = 1, 0$ eigenstate at \mathbf{k}_p ,

$$f_n(\mathbf{k}_p, \mathbf{r}) = \langle \mathbf{r} | f_n(\mathbf{k}_p) \rangle = \mathbf{e} c_n(\mathbf{k}_p, \mathbf{r}). \quad (54)$$

$c_n(\mathbf{k}_p, \mathbf{r} + \mathbf{R}) = c_n(\mathbf{k}_p, \mathbf{r})$ is some arbitrary periodic scalar function. This is an incredibly convenient simplification and implies the precise coordinates of the matter oscillations ψ_α are superfluous at these points in the Brillouin zone. In Sec. IV we will connect these rotational eigenvalues directly to the Chern number.

IV. TOPOLOGICAL ELECTROMAGNETIC (BOSONIC) PHASES OF MATTER

A. Electromagnetic Chern number

The Berry connection for a band n is found by varying the total Bloch wave function $|u_{n\mathbf{k}}\rangle$ with respect to the momentum,

$$\mathbf{A}_n(\mathbf{k}) = -i \langle u_{n\mathbf{k}} | \partial_{\mathbf{k}} u_{n\mathbf{k}} \rangle = -i \sum_{\mathbf{g}} u_{n\mathbf{k}+\mathbf{g}}^\dagger \partial_{\mathbf{k}} u_{n\mathbf{k}+\mathbf{g}}. \quad (55)$$

This can be simplified slightly to obtain,

$$\begin{aligned} \mathbf{A}_n(\mathbf{k}) = & -i \sum_{\mathbf{g}\mathbf{g}'} f_{n\mathbf{k}+\mathbf{g}}^\dagger \bar{\mathcal{M}}_{\mathbf{g}'-\mathbf{g}}(\omega_{n\mathbf{k}}, \mathbf{k} + \mathbf{g}) \partial_{\mathbf{k}} f_{n\mathbf{k}+\mathbf{g}'} \\ & + \sum_{\mathbf{g}\mathbf{g}'} f_{n\mathbf{k}+\mathbf{g}}^\dagger \mathcal{A}_{\mathbf{g}'-\mathbf{g}}(\omega_{n\mathbf{k}}, \mathbf{k} + \mathbf{g}) f_{n\mathbf{k}+\mathbf{g}'}. \end{aligned} \quad (56)$$

The first term gives the Berry connection of the photon, while the second term $\mathcal{A}_{\mathbf{g}}(\omega, \mathbf{k})$ arises solely from the matter oscillations,

$$\mathcal{A}_{\mathbf{g}}(\omega, \mathbf{k}) = -i \sum_{\alpha\mathbf{g}'} \frac{\mathcal{C}_{\alpha-\mathbf{g}'}^\dagger(\mathbf{k} + \mathbf{g}') \partial_{\mathbf{k}} \mathcal{C}_{\alpha\mathbf{g}-\mathbf{g}'}(\mathbf{k} + \mathbf{g}')}{(\omega - \omega_{\alpha\mathbf{k}+\mathbf{g}'})^2}. \quad (57)$$

Due to nonlocality, Eq. (57) does not generally vanish. This additional contribution to the Berry phase corresponds to vortices in the response function itself - independent of the Berry gauge of the photon. This means the Chern number can be nonzero $\mathfrak{C}_n \neq 0$ even if the winding of electromagnetic field is trivial. However, we will show in the proceeding sections that all symmetry constraints on the Chern number can be established entirely in terms of the photon.

As can be seen from Eq. (56), the Berry connection is only defined within the Brillouin zone $\mathbf{A}_{n\mathbf{k}+\mathbf{g}} = \mathbf{A}_{n\mathbf{k}} + \partial_{\mathbf{k}} \chi_{n\mathbf{k}}$, up to a possible U(1) gauge. Hence, the gauge invariant Berry curvature is periodic $F_{n\mathbf{k}+\mathbf{g}} = F_{n\mathbf{k}}$,

$$F_n(\mathbf{k}) = \hat{\mathbf{z}} \cdot [\partial_{\mathbf{k}} \times \mathbf{A}_n(\mathbf{k})]. \quad (58)$$

The Chern number is found by integrating the Berry curvature over the two-dimensional Brillouin zone,

$$\mathfrak{C}_n = \frac{1}{2\pi} \int_{\text{BZ}} F_n(\mathbf{k}) d^2\mathbf{k}, \quad \mathfrak{C}_n \in \mathbb{Z}, \quad (59)$$

which determines the winding number of the collective light-matter excitations over the torus $\mathbb{T}^2 = S^1 \times S^1$. Equation (59) is one of the central results of this paper. An electromagnetic Chern invariant can be found for any 2D crystal and characterizes distinct topological bosonic phases of matter $\mathfrak{C}_n \neq 0$.

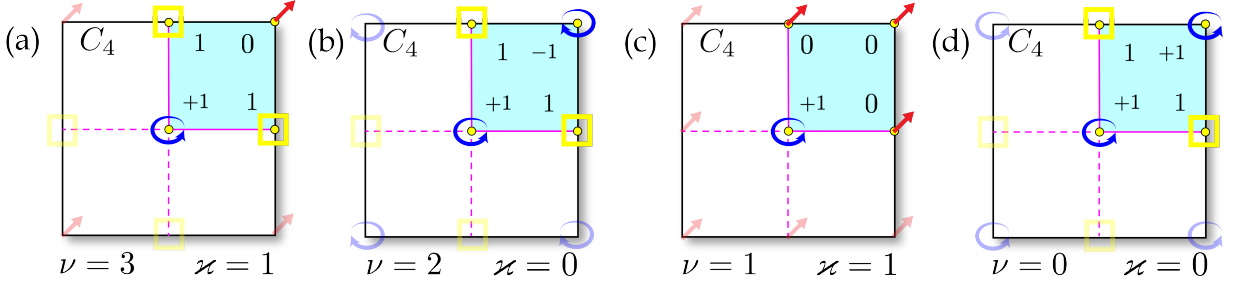


FIG. 3. Examples of SPT bosonic phases in a crystal with C_4 symmetry. The photon possesses quantized spin $m = \pm 1, 0$ or inversion $p = 1, 0$ eigenvalues at HSPs. These phases are characterized by their SPT invariant $\nu = m(\Gamma) + m(M) + 2p(Y) \pmod 4$ which determines the electromagnetic Chern number up to a multiple of 4. The inversion invariant $\varkappa = p(\Gamma) + p(M) \pmod 2$ determines the parity of the Chern number (odd or even). (a), (b), (c) and (d) correspond to SPT bosonic phases of $\nu = 3, 2, 1$ and 0 respectively. For instance, the $\nu = 2$ and $\varkappa = 0$ phase has spin eigenvalues of $m(\Gamma) = +1$ at the center and $m(M) = -1$ at the vertices, with inversion eigenvalues of $p(Y) = p(X) = 1$ at the edge centers. Notice there is a net change in spin of $\Delta m = 2$ from Γ to M but the magnitude $|m| = 1$ is unchanged. This phase represents spin precession. All other nontrivial phases have $\Delta m = 1$ which requires a change in magnitude for spin-1.

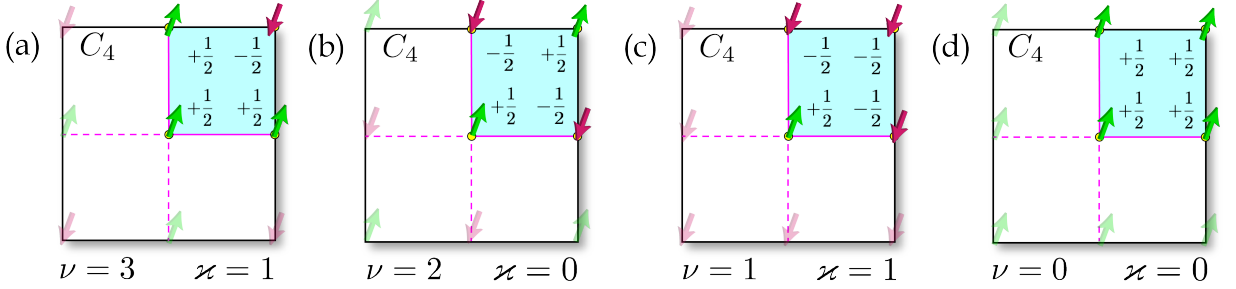


FIG. 4. Examples of SPT fermionic phases in a crystal with C_4 symmetry. The electron possesses quantized spin- $1/2$ eigenvalues $m = \pm 1/2$ at HSPs. These phases are characterized by their SPT invariant $\nu = m(\Gamma) + m(M) + 2m(Y) + 2 \pmod 4$ which determines the electronic Chern number up to a multiple of 4. The inversion invariant $\varkappa = m(\Gamma) + m(M) + 1 \pmod 2$ determines the parity of the Chern number (odd or even). (a), (b), (c) and (d) correspond to SPT fermionic phases of $\nu = 3, 2, 1$ and 0 respectively. For example, the $\nu = 2$ and $\varkappa = 0$ phase has spin eigenvalues of $m(\Gamma) = m(M) = +1/2$ at the center and vertices, with $m(Y) = m(X) = -1/2$ at the edge centers. This particular phase is very different from its bosonic counterpart. For the fermion, there is no net change in spin $\Delta m = 0$ from Γ to M - a change of $\Delta m = 2$ is impossible for a spin- $1/2$ particle. All other nontrivial phases have $\Delta m = 1$, which is possible for both spin- $1/2$ and spin-1. However, all fermionic phases represent spin precession since the magnitude $|m| = 1/2$ cannot change for a spin- $1/2$ particle.

B. Symmetry-protected topological bosonic phases

Nevertheless, even if we knew the specifics of the material, evaluating the Chern number by brute force would be a herculean task. Instead, we invoke constraints of the point groups, which constitute a type of *symmetry-protected topological* (SPT) phase [60–69]. SPT phases are protected by the N -fold rotational symmetry of C_N and this gives rise to an additional topological invariant $\nu_n \in \mathbb{Z}_N$. Remarkably, ν_n is classified entirely from $z_n(\mathbf{k}_p)$ eigenvalues at HSPs and requires no complicated integration to compute. This invariant is related to the Chern number up to a multiple of N ,

$$\nu_n = \mathfrak{C}_n \pmod N, \quad \mathfrak{C}_n \in N\mathbb{Z} + \nu_n. \quad (60)$$

The interpretation of ν_n is quite simple - it tells us the geometric phase around the irreducible Brillouin zone (IBZ) of the crystal,

$$\begin{aligned} \exp\left(i\frac{2\pi}{N}\mathfrak{C}_n\right) &= \exp\left(i\int_{\text{IBZ}} F_n(\mathbf{k})d^2\mathbf{k}\right) \\ &= \exp\left(i\oint_{\partial\text{IBZ}} \mathbf{A}_n(\mathbf{k}) \cdot d\mathbf{k}\right), \end{aligned} \quad (61)$$

where ∂IBZ is the path around IBZ. For instance, the path in C_4 is $\partial(\text{IBZ})_4 = \Gamma\text{XMY}\Gamma$. Applying the logarithm, ν_n is equivalent to,

$$\nu_n = \frac{N}{2\pi} \oint_{\partial\text{RBZ}} \mathbf{A}_n(\mathbf{k}) \cdot d\mathbf{k} \pmod N. \quad (62)$$

As we will see more explicitly, ν_n is tied entirely to spin. The reason is subtle - any vortex within the interior of the IBZ contributes a Berry phase of 2π , and by symmetry, there are N such vortices within the total Brillouin zone $\mathfrak{C}_n \rightarrow \mathfrak{C}_n + N$. However, this has no effect on $\nu_n \rightarrow \nu_n$. Only the vortices lying at HSPs contribute to ν_n because these come in fractions of 2π .

We also introduce one additional topological invariant $\varkappa_n \in \mathbb{Z}_2$ for crystals with inversion symmetry $C_{N=2,4,6}$. The inversion invariant determines the parity of the electromagnetic Chern number (odd or even),

$$\varkappa_n = \mathfrak{C}_n \pmod 2. \quad (63)$$

The parity of \mathfrak{C}_n turns out to be incredibly important in bosonic systems and has very different interpretations than

their fermionic counterparts. This is because the bosonic Chern number does not necessarily count the number of edge states [11–19] - something we might expect from fermionic arguments.

In the following sections we will discuss the bosonic classification of ν_n and \varkappa_n for each cyclic point group and the SPT phases associated with them. We do not present the full derivations here since the rigorous proofs have been carried out by others (see Ref. [63]) - we simply state the salient results. For completeness, in Appendix A we also discuss the SPT *fermionic* phases associated with each point group. We do this to emphasize that fermionic and bosonic systems represent distinct topological field theories, with fundamentally different interpretations. These differences are highlighted with a few examples.

C. Twofold (inversion) symmetry: C_2

For the C_2 point group, or simply inversion symmetry, the SPT phase is related to the Chern number by $\nu_n = \varkappa_n = \mathfrak{C}_n \pmod 2$ which is a \mathbb{Z}_2 invariant. There is only one nontrivial phase and it can be found modulo 2 from,

$$\exp\left(i\frac{2\pi}{2}\mathfrak{C}_n\right) = z_{2,n}(\Gamma)z_{2,n}(\text{X})z_{2,n}(\text{Y})z_{2,n}(\text{M}). \quad (64)$$

Applying the logarithm, this classification can be expressed equivalently in terms of $p_n = 1, 0$ inversion eigenvalues,

$$\nu_n = \varkappa_n = p_n(\Gamma) + p_n(\text{X}) + p_n(\text{Y}) + p_n(\text{M}) \pmod 2. \quad (65)$$

If the summation of eigenvalues is odd, the SPT phase is nontrivial $\nu_n = \varkappa_n = 1$ and corresponds to an odd-valued Chern number. Clearly this is only possible when magnetic resonances are present $p_n = 0$. If the material is *nonmagnetic*, the SPT phase is always trivial $\nu_n = \varkappa_n = 0$ and odd-valued Chern numbers are *forbidden*. As we will see, all crystals with inversion symmetry $C_{N=2,4,6}$ possess this strict constraint.

D. Threefold symmetry: C_3

C_3 is unique in this respect because it is the only point group with an odd rotational symmetry - i.e. it lacks inversion symmetry. This means the parity of Chern number (odd or even) is not restricted by the symmetries of the crystal. For C_3 , the SPT phase is $\nu_n = \mathfrak{C}_n \pmod 3$ which is a \mathbb{Z}_3 invariant. There are two nontrivial phases and they can be found modulo 3 from,

$$\exp\left(i\frac{2\pi}{3}\mathfrak{C}_n\right) = z_{3,n}(\Gamma)z_{3,n}(\text{K})z_{3,n}(\text{K}'). \quad (66)$$

This classification is expressed equivalently in terms of quantized spin eigenvalues $m_n = \pm 1, 0$ at HSPs,

$$\nu_n = m_n(\Gamma) + m_n(\text{K}) + m_n(\text{K}') \pmod 3. \quad (67)$$

In this point group, the phase is only nontrivial $\nu_n \neq 0$ if the spin eigenvalues differ at HSPs. Note though, odd and even

phases are not distinct $-2 = 1 = 4$ under modulo 3. C_3 is the only point group besides C_1 that permits odd-valued Chern numbers in nonmagnetic materials.

E. Fourfold symmetry: C_4

For the C_4 point group, the SPT phase is related to the Chern number by $\nu_n = \mathfrak{C}_n \pmod 4$ which is a \mathbb{Z}_4 invariant. There are three nontrivial phases and they can be found modulo 4 from,

$$\exp\left(i\frac{2\pi}{4}\mathfrak{C}_n\right) = z_{4,n}(\Gamma)z_{4,n}(\text{M})z_{2,n}(\text{Y}). \quad (68)$$

The classification is expressed equivalently in terms of spin and inversion eigenvalues,

$$\nu_n = m_n(\Gamma) + m_n(\text{M}) + 2p_n(\text{Y}) \pmod 4. \quad (69)$$

Moreover, the parity of the phase $\varkappa_n = \mathfrak{C}_n \pmod 2$ can be found by squaring Eq. (68) and using properties of the roots $z_2 = z_4^2$,

$$\exp\left(i\frac{2\pi}{2}\mathfrak{C}_n\right) = z_{2,n}(\Gamma)z_{2,n}(\text{M}). \quad (70)$$

This is identical to the inversion eigenvalues at the center and vertices of the Brillouin zone,

$$\varkappa_n = p_n(\Gamma) + p_n(\text{M}) \pmod 2. \quad (71)$$

Again, we see that $\varkappa_n = 1$ phases (odd-valued Chern numbers) are only possible in magnetic materials. Examples of all C_4 SPT bosonic phases are presented in Fig. 3 and these are compared with their fermionic counterparts in Fig. 4.

F. Sixfold symmetry: C_6

For the C_6 point group, the SPT phase is $\nu_n = \mathfrak{C}_n \pmod 6$ which is a \mathbb{Z}_6 invariant. There are five nontrivial phases and they can be found modulo 6 from,

$$\exp\left(i\frac{2\pi}{6}\mathfrak{C}_n\right) = z_{6,n}(\Gamma)z_{3,n}(\text{K})z_{2,n}(\text{M}). \quad (72)$$

This is equivalent to the summation of spin and inversion eigenvalues,

$$\nu_n = m_n(\Gamma) + 2m_n(\text{K}) + 3p_n(\text{M}) \pmod 6. \quad (73)$$

The parity of the phase $\varkappa_n = \mathfrak{C}_n \pmod 2$, can be found by cubing Eq. (72) and using the fact that $z_2 = z_6^3 = z_2^3$,

$$\exp\left(i\frac{2\pi}{2}\mathfrak{C}_n\right) = z_{2,n}(\Gamma)z_{2,n}(\text{M}). \quad (74)$$

Like C_4 , we can express this in terms of inversion eigenvalues at the Γ and M points,

$$\varkappa_n = p_n(\Gamma) + p_n(\text{M}) \pmod 2. \quad (75)$$

This completes the classification of all 2+1D topological electromagnetic (bosonic) phases of matter which is summarized in Tbl. I. These are compared alongside their fermionic counterparts in Tbl. II.

G. Continuous symmetry: C_∞

To finish, we briefly discuss the continuum limit $\mathbf{g} = 0$ and the topological phases that can be described by a long wavelength theory $k \approx 0$. The physics is significantly more tractable here and exactly solvable models are possible (see Ref. [22, 23]). In this limit, the rotational symmetry of the crystal is approximately continuous C_∞ . The SPT invariant ν_n and Chern number \mathfrak{C}_n are thus equivalent,

$$\nu_n = \mathfrak{C}_n = m_n(0) - m_n(\infty). \quad (76)$$

Note that $\nu_n \in \mathbb{Z}$ is not a modulo integer in this limit and does not have the same interpretation as the lattice theory. Clearly though, the spin eigenstates must change at HSPs $m_n(0) \neq m_n(\infty)$ for a nontrivial phase to exist $\mathfrak{C}_n \neq 0$. In the continuum regularization, $k_p = 0$ represents the Γ point and $k_p = \infty$ is interpreted as mapping the vertices of the Brillouin zone into one another.

Nonetheless, the continuum theory has a few limitations which are not present in the full lattice theory. First, it can only approximate crystals that possess a definite center, i.e. are at least threefold cyclic. Even this is not entirely accurate because C_3 lacks inversion symmetry, which cannot be accounted for in the $\mathbf{g} = 0$ harmonic. Second, the continuum Chern number has strictly two phases $\mathfrak{C}_n = \pm 2, \pm 1$, while the lattice theory has no such restrictions $\mathfrak{C}_n \in \mathbb{Z}$. This is because all higher-order harmonics $\mathbf{g} \neq 0$ can, in principle, contribute an arbitrary number of vortices to the Berry phase.

V. CONCLUSIONS

In summary, we have developed the complete 2+1D lattice field theory describing all symmetry-protected topological bosonic phases of the photon. To accomplish this, we analyzed the electromagnetic Bloch waves in microscopic crystals and derived the Chern invariant of these light-matter excitations. Thereafter, the rotational symmetries of the crystal were examined extensively and the implications these have on photonic spin. We have studied all two dimensional point groups C_N with nonvanishing Chern number and linked the topological invariants directly to spin-1 quantized eigenvalues of the electromagnetic field - establishing the bosonic classification for each topological phase. A strong constraint of this classification is that odd-valued Chern numbers are forbidden in nonmagnetic materials with inversion symmetry $C_{N=2,4,6}$.

ACKNOWLEDGEMENTS

This research was supported by the Defense Advanced Research Projects Agency (DARPA) Nascent Light-Matter Interactions (NLM) Program and the National Science Foundation (NSF) [Grant No. EFMA-1641101].

APPENDIX

Appendix A: Symmetry-protected topological fermionic phases

For completeness, we examine the SPT fermionic phases associated with each point group C_N and highlight their es-

sential differences from bosons. The most important distinction is how they transform under rotations; half-integer particles are antisymmetric $\mathcal{R}(2\pi) = -1$. In terms of discrete rotations \mathcal{R}_N about the z -axis, the eigenstates of a spin- $1/2$ particle (free electron) satisfy,

$$\mathcal{R}_N|\Psi\rangle = w_N|\Psi\rangle, \quad \hat{S}_z|\Psi\rangle = m|\Psi\rangle, \quad (A1)$$

where the eigenvalues related by,

$$w_N = \exp(i\theta_N m), \quad (w_N)^N = -1, \quad (A2)$$

and $\theta_N = 2\pi/N$ is an N -fold rotation. Notice that w_N represents the N th root of *negative* unity because the spin is half-integer $m = \pm 1/2$, and unlike the photon, there are only two spin degrees of freedom. The dimensionality of the problem plays a key role in the topology. For example, right- and left-handed spin-1 states $m = \pm 1$ have identical inversion eigenvalues. On the contrary, up and down spin- $1/2$ states $m = \pm 1/2$ have *opposite* inversion eigenvalues,

$$\mathcal{R}_2|\Psi\rangle = \hat{P}|\Psi\rangle = w_2|\Psi\rangle, \quad w_2 = (-1)^m = \pm i. \quad (A3)$$

This is because a rotation by π and $-\pi$ is not equivalent for fermions.

The single-particle fermionic classification for C_2, C_3, C_4 and C_6 respectively is [63, 68],

$$\exp\left(i\frac{2\pi}{2}\mathfrak{C}\right) = w_2(\Gamma)w_2(\mathbf{X})w_2(\mathbf{Y})w_2(\mathbf{M}), \quad (A4a)$$

$$\exp\left(i\frac{2\pi}{3}\mathfrak{C}\right) = -w_3(\Gamma)w_3(\mathbf{K})w_3(\mathbf{K}'), \quad (A4b)$$

$$\exp\left(i\frac{2\pi}{4}\mathfrak{C}\right) = -w_4(\Gamma)w_4(\mathbf{M})w_2(\mathbf{Y}), \quad (A4c)$$

$$\exp\left(i\frac{2\pi}{6}\mathfrak{C}\right) = -w_6(\Gamma)w_3(\mathbf{K})w_2(\mathbf{M}). \quad (A4d)$$

Although the classification appears similar, the SPT fermionic phases constitute very different physics than their bosonic counterparts, which is alluded to by the antisymmetric phase factors $\mathcal{R}(2\pi) = -1$. We illustrate this with an example in C_4 . Applying the logarithm - the classification for the SPT fermionic phase $\nu = \mathfrak{C} \bmod 4$ can be expressed as,

$$\nu = m(\Gamma) + m(\mathbf{M}) + 2m(\mathbf{Y}) + 2 \bmod 4, \quad (A5)$$

where $m = \pm 1/2$ are half-integer eigenvalues. The parity of the phase $\varkappa = \mathfrak{C} \bmod 2$ reads,

$$\varkappa = m(\Gamma) + m(\mathbf{M}) + 1 \bmod 2, \quad (A6)$$

which follows from $w_4^2 = w_2$ and $w_2^2 = -1$.

- [1] M. Z. Hasan and C. L. Kane, “Colloquium: Topological insulators,” *Rev. Mod. Phys.* **82**, 3045–3067 (2010).
- [2] F. D. M. Haldane, “Model for a quantum hall effect without landau levels: Condensed-matter realization of the “parity anomaly”,” *Phys. Rev. Lett.* **61**, 2015–2018 (1988).
- [3] D Jaksch and P Zoller, “Creation of effective magnetic fields in optical lattices: the hofstadter butterfly for cold neutral atoms,” *New Journal of Physics* **5**, 56 (2003).
- [4] Jens Koch, Andrew A. Houck, Karyn Le Hur, and S. M. Girvin, “Time-reversal-symmetry breaking in circuit-qed-based photon lattices,” *Phys. Rev. A* **82**, 043811 (2010).
- [5] Gregor Jotzu, Michael Messer, Rémi Desbuquois, Martin Lebrat, Thomas Uehlinger, Daniel Greif, and Tilman Esslinger, “Experimental realization of the topological haldane model with ultracold fermions,” *Nature* **515**, 237 EP – (2014).
- [6] C. L. Kane and E. J. Mele, “Quantum spin hall effect in graphene,” *Phys. Rev. Lett.* **95**, 226801 (2005).
- [7] B. Andrei Bernevig, Taylor L. Hughes, and Shou-Cheng Zhang, “Quantum spin hall effect and topological phase transition in hgte quantum wells,” *Science* **314**, 1757–1761 (2006).
- [8] K. v. Klitzing, G. Dorda, and M. Pepper, “New method for high-accuracy determination of the fine-structure constant based on quantized hall resistance,” *Phys. Rev. Lett.* **45**, 494–497 (1980).
- [9] R. B. Laughlin, “Quantized hall conductivity in two dimensions,” *Phys. Rev. B* **23**, 5632–5633 (1981).
- [10] D. J. Thouless, M. Kohmoto, M. P. Nightingale, and M. den Nijs, “Quantized hall conductance in a two-dimensional periodic potential,” *Phys. Rev. Lett.* **49**, 405–408 (1982).
- [11] Xie Chen, Zheng-Xin Liu, and Xiao-Gang Wen, “Two-dimensional symmetry-protected topological orders and their protected gapless edge excitations,” *Phys. Rev. B* **84**, 235141 (2011).
- [12] Xie Chen, Zheng-Cheng Gu, Zheng-Xin Liu, and Xiao-Gang Wen, “Symmetry-protected topological orders in interacting bosonic systems,” *Science* **338**, 1604–1606 (2012).
- [13] Yuan-Ming Lu and Ashvin Vishwanath, “Theory and classification of interacting integer topological phases in two dimensions: A chern-simons approach,” *Phys. Rev. B* **86**, 125119 (2012).
- [14] Ashvin Vishwanath and T. Senthil, “Physics of three-dimensional bosonic topological insulators: Surface-deconfined criticality and quantized magnetoelectric effect,” *Phys. Rev. X* **3**, 011016 (2013).
- [15] Max A. Metlitski, C. L. Kane, and Matthew P. A. Fisher, “Bosonic topological insulator in three dimensions and the statistical witten effect,” *Phys. Rev. B* **88**, 035131 (2013).
- [16] T. Senthil and Michael Levin, “Integer quantum hall effect for bosons,” *Phys. Rev. Lett.* **110**, 046801 (2013).
- [17] Zeren Lin and Zhirong Liu, “Spin-1 dirac-weyl fermions protected by bipartite symmetry,” *The Journal of Chemical Physics* **143**, 214109 (2015).
- [18] Tian Lan, Liang Kong, and Xiao-Gang Wen, “Theory of (2+1)-dimensional fermionic topological orders and fermionic/bosonic topological orders with symmetries,” *Phys. Rev. B* **94**, 155113 (2016).
- [19] Tiantian Zhang, Zhida Song, A. Alexandradinata, Hongming Weng, Chen Fang, Ling Lu, and Zhong Fang, “Double-weyl phonons in transition-metal monosilicides,” *Phys. Rev. Lett.* **120**, 016401 (2018).
- [20] Y. Ikebe, T. Morimoto, R. Masutomi, T. Okamoto, H. Aoki, and R. Shimano, “Optical hall effect in the integer quantum hall regime,” *Phys. Rev. Lett.* **104**, 256802 (2010).
- [21] Yisong Zheng and Tsuneya Ando, “Hall conductivity of a two-dimensional graphite system,” *Phys. Rev. B* **65**, 245420 (2002).
- [22] Todd Van Mechelen and Zubin Jacob, “Quantum gyroelectric effect: Photon spin-1 quantization in continuum topological bosonic phases,” *Phys. Rev. A* **98**, 023842 (2018).
- [23] Todd Van Mechelen and Zubin Jacob, “Photonic Dirac monopoles and skyrmions: spin-1 quantization,” arXiv:1806.09879 (2018).
- [24] G. V. Dunne, “Aspects of chern-simons theory,” in *Aspects topologiques de la physique en basse dimension. Topological aspects of low dimensional systems*, edited by A. Comtet, T. Jolicœur, S. Ouvry, and F. David (Springer Berlin Heidelberg, Berlin, Heidelberg, 1999) pp. 177–263.
- [25] D. Boyanovsky, R. Blankenbecler, and R. Yahalom, “Physical origin of topological mass in 2 + 1 dimensions,” *Nuclear Physics B* **270**, 483 – 505 (1986).
- [26] S. A. R. Horsley, “Topology and the optical dirac equation,” *Phys. Rev. A* **98**, 043837 (2018).
- [27] S. Raghu and F. D. M. Haldane, “Analogues of quantum-hall-effect edge states in photonic crystals,” *Phys. Rev. A* **78**, 033834 (2008).
- [28] F. D. M. Haldane and S. Raghu, “Possible realization of directional optical waveguides in photonic crystals with broken time-reversal symmetry,” *Phys. Rev. Lett.* **100**, 013904 (2008).
- [29] Zheng Wang, Yidong Chong, J. D. Joannopoulos, and Marin Soljacic, “Observation of unidirectional backscattering-immune topological electromagnetic states,” *Nature* **461**, 772–775 (2009).
- [30] Zheng Wang and Shanhui Fan, “Optical circulators in two-dimensional magneto-optical photonic crystals,” *Opt. Lett.* **30**, 1989–1991 (2005).
- [31] Ling Lu, Liang Fu, John D. Joannopoulos, and Marin Soljacic, “Weyl points and line nodes in gyroid photonic crystals,” *Nat Photon* **7**, 294–299 (2013).
- [32] M. Hafezi, S. Mittal, J. Fan, A. Migdall, and J. M. Taylor, “Imaging topological edge states in silicon photonics,” *Nat Photon* **7**, 1001–1005 (2013), article.
- [33] Zheng-Cheng Gu, Zhenhan Wang, and Xiao-Gang Wen, “Classification of two-dimensional fermionic and bosonic topological orders,” *Phys. Rev. B* **91**, 125149 (2015).
- [34] Torsten Karzig, Charles-Edouard Bardyn, Netanel H. Lindner, and Gil Refael, “Topological polaritons,” *Phys. Rev. X* **5**, 031001 (2015).
- [35] Yakir Hadad, Vincenzo Vitelli, and Andrea Alu, “Solitons and propagating domain walls in topological resonator arrays,” *ACS Photonics* **4**, 1974–1979 (2017).
- [36] Giuseppe De Nittis and Max Lein, “Symmetry Classification of Topological Photonic Crystals,” arXiv:1710.08104 (2017).
- [37] Netanel H. Lindner, Gil Refael, and Victor Galitski, “Floquet topological insulator in semiconductor quantum wells,” *Nature Physics* **7**, 490 EP – (2011), article.
- [38] Jerome Cayssol, Balazs Dora, Ferenc Simon, and Roderich Moessner, “Floquet topological insulators,” *physica status solidi (RRL) Rapid Research Letters* **7**, 101–108 (2013).
- [39] Mikael C. Rechtsman, Julia M. Zeuner, Yonatan Plotnik, Yaakov Lumer, Daniel Podolsky, Felix Dreisow, Stefan Nolte, Mordechai Segev, and Alexander Szameit, “Photonic floquet topological insulators,” *Nature* **496**, 196–200 (2013), letter.
- [40] Alexander B. Khanikaev and Gennady Shvets, “Two-dimensional topological photonics,” *Nature Photonics* **11**, 763–

- 773 (2017).
- [41] Alexey Slobozhanyuk, S. Hossein Mousavi, Xiang Ni, Daria Smirnova, Yuri S. Kivshar, and Alexander B. Khanikaev, “Three-dimensional all-dielectric photonic topological insulator,” *Nat Photon* **11**, 130–136 (2017), article.
- [42] Cheng He, Xiao-Chen Sun, Xiao-Ping Liu, Ming-Hui Lu, Yulin Chen, Liang Feng, and Yan-Feng Chen, “Photonic topological insulator with broken time-reversal symmetry,” *Proceedings of the National Academy of Sciences* **113**, 4924–4928 (2016).
- [43] I. V. Lindell and A. H. Sihvola, “Realization of the pemc boundary,” *IEEE Transactions on Antennas and Propagation* **53**, 3012–3018 (2005).
- [44] Junfei Li, Chen Shen, Ana Díaz-Rubio, Sergei A. Tretyakov, and Steven A. Cummer, “Systematic design and experimental demonstration of bianisotropic metasurfaces for scattering-free manipulation of acoustic wavefronts,” *Nature Communications* **9**, 1342 (2018).
- [45] Yu Guo, Meng Xiao, and Shanhui Fan, “Topologically protected complete polarization conversion,” *Phys. Rev. Lett.* **119**, 167401 (2017).
- [46] Kun Ding, Guancong Ma, Meng Xiao, Z. Q. Zhang, and C. T. Chan, “Emergence, coalescence, and topological properties of multiple exceptional points and their experimental realization,” *Phys. Rev. X* **6**, 021007 (2016).
- [47] Mário G. Silveirinha, “Chern invariants for continuous media,” *Phys. Rev. B* **92**, 125153 (2015).
- [48] Wenlong Gao, Mark Lawrence, Biao Yang, Fu Liu, Fengzhou Fang, Benjamin Béri, Jensen Li, and Shuang Zhang, “Topological photonic phase in chiral hyperbolic metamaterials,” *Phys. Rev. Lett.* **114**, 037402 (2015).
- [49] Dafei Jin, Ling Lu, Zhong Wang, Chen Fang, John D. Joannopoulos, Marin Soljacic, Liang Fu, and Nicholas X. Fang, “Topological magnetoplasmon,” *Nature Communications* **7**, 13486 EP – (2016), article.
- [50] S. A. Hassani Gangaraj, M. G. Silveirinha, and G. W. Hanson, “Berry phase, berry connection, and chern number for a continuum bianisotropic material from a classical electromagnetics perspective,” *IEEE Journal on Multiscale and Multiphysics Computational Techniques* **2**, 3–17 (2017).
- [51] Li-kun Shi and Justin C. W. Song, “Plasmon geometric phase and plasmon hall shift,” *Phys. Rev. X* **8**, 021020 (2018).
- [52] Iwo Bialynicki-Birula and Zofia Bialynicka-Birula, “Berry’s phase in the relativistic theory of spinning particles,” *Phys. Rev. D* **35**, 2383–2387 (1987).
- [53] Michael Stone, “Berry phase and anomalous velocity of weyl fermions and maxwell photons,” *International Journal of Modern Physics B* **30**, 1550249 (2016).
- [54] O. El Gawhary, T. Van Mechelen, and H. P. Urbach, “Role of radial charges on the angular momentum of electromagnetic fields: Spin-3/2 light,” *Phys. Rev. Lett.* **121**, 123202 (2018).
- [55] J Hubbard, “The dielectric theory of electronic interactions in solids,” *Proceedings of the Physical Society. Section A* **68**, 976 (1955).
- [56] David S. Falk, “Effect of the lattice on dielectric properties of an electron gas,” *Phys. Rev.* **118**, 105–109 (1960).
- [57] David R. Penn, “Wave-number-dependent dielectric function of semiconductors,” *Phys. Rev.* **128**, 2093–2097 (1962).
- [58] Lev Davidovich Landau, JS Bell, MJ Kearsley, LP Pitaevskii, EM Lifshitz, and JB Sykes, *Electrodynamics of Continuous Media*, Vol. 8 (Elsevier, New York, 2013).
- [59] Vladimir M Agranovich and Vitaly Ginzburg, *Crystal optics with spatial dispersion, and excitons*, Vol. 42 (Springer Science & Business Media, New York, 2013).
- [60] Liang Fu, “Topological crystalline insulators,” *Phys. Rev. Lett.* **106**, 106802 (2011).
- [61] Taylor L. Hughes, Emil Prodan, and B. Andrei Bernevig, “Inversion-symmetric topological insulators,” *Phys. Rev. B* **83**, 245132 (2011).
- [62] Robert-Jan Slager, Andrej Mesaros, Vladimir Juricic, and Jan Zaenen, “The space group classification of topological band-insulators,” *Nature Physics* **9**, 98 EP – (2012), article.
- [63] Chen Fang, Matthew J. Gilbert, and B. Andrei Bernevig, “Bulk topological invariants in noninteracting point group symmetric insulators,” *Phys. Rev. B* **86**, 115112 (2012).
- [64] Barry Bradlyn, L. Elcoro, Jennifer Cano, M. G. Vergniory, Zhi-jun Wang, C. Felser, M. I. Aroyo, and B. Andrei Bernevig, “Topological quantum chemistry,” *Nature* **547**, 298 EP – (2017), article.
- [65] Hao Song, Sheng-Jie Huang, Liang Fu, and Michael Hermele, “Topological phases protected by point group symmetry,” *Phys. Rev. X* **7**, 011020 (2017).
- [66] Hoi Chun Po, Ashvin Vishwanath, and Haruki Watanabe, “Symmetry-based indicators of band topology in the 230 space groups,” *Nature Communications* **8**, 50 (2017).
- [67] Ryan Thorngren and Dominic V. Else, “Gauging spatial symmetries and the classification of topological crystalline phases,” *Phys. Rev. X* **8**, 011040 (2018).
- [68] Akishi Matsugatani, Yuri Ishiguro, Ken Shiozaki, and Haruki Watanabe, “Universal relation among the many-body chern number, rotation symmetry, and filling,” *Phys. Rev. Lett.* **120**, 096601 (2018).
- [69] Haruki Watanabe, Hoi Chun Po, and Ashvin Vishwanath, “Structure and topology of band structures in the 1651 magnetic space groups,” *Science Advances* **4** (2018), 10.1126/sciadv.aat8685.
- [70] Todd Van Mechelen and Zubin Jacob, “Dirac-Maxwell correspondence: Spin-1 bosonic topological insulator,” arXiv: 1708.08192 (2017).
- [71] Xiaobo Yin, Ziliang Ye, Junsuk Rho, Yuan Wang, and Xiang Zhang, “Photonic spin hall effect at metasurfaces,” *Science* **339**, 1405–1407 (2013).
- [72] Todd Van Mechelen and Zubin Jacob, “Universal spin-momentum locking of evanescent waves,” *Optica* **3**, 118–126 (2016).
- [73] Farid Kalhor, Thomas Thundat, and Zubin Jacob, “Universal spin-momentum locked optical forces,” *Applied Physics Letters* **108**, 061102 (2016).
- [74] Sarang Pendharker, Farid Kalhor, Todd Van Mechelen, Saman Jahani, Neda Nazemifard, Thomas Thundat, and Zubin Jacob, “Spin photonic forces in non-reciprocal waveguides,” *Opt. Express* **26**, 23898–23910 (2018).
- [75] Konstantin Y. Bliokh, Daria Smirnova, and Franco Nori, “Quantum spin hall effect of light,” *Science* **348**, 1448–1451 (2015).
- [76] Max Born and Kun Huang, *Dynamical theory of crystal lattices* (Clarendon Press, Oxford, 1954).
- [77] S A R Horsley and T G Philbin, “Canonical quantization of electromagnetism in spatially dispersive media,” *New Journal of Physics* **16**, 013030 (2014).
- [78] David Hestenes, “Point groups and space groups in geometric algebra,” in *Applications of Geometric Algebra in Computer Science and Engineering*, edited by Leo Dorst, Chris Doran, and Joan Lasenby (Birkhäuser Boston, Boston, MA, 2002) pp. 3–34.
- [79] John Frederick Nye, *Physical properties of crystals: their representation by tensors and matrices* (Oxford University Press, New York, 1985).